Visnyk NTUU KPI Seriia – Radiotekhnika Radioaparatobuduvannia, 2026, Iss. 104, pp. 23–32

UDC 621.396, 621.3.049

Hybrid-Integrated Balanced Subharmonic Mixer of the Millimeter Range With Low Conversion Losses

Omelianenko M. Yu., Romanenko T. V., Turieieva O. V.

National Technical University of Ukraine "Ihor Sikorsky Kyiv Polytechnic Institute", Kyiv, Ukraine

E-mail: *hohner_@ukr.net*

The paper comprehensively investigates the proposed topology of a hybrid-integrated circuit of a balanced subharmonic mixer, effective when used in the millimeter wavelength range. The principle of operation of the mixer is covered in detail, its model is proposed in terms of the theory of long lines, on the basis of which the dimensions of the elements of the topology of the integrated circuit are calculated in the first approximation. The dimensions are refined in the electrodynamic analysis program CST Microwave Studio. According to the results of the calculations, mixer samples were manufactured and their experimental study was conducted. The process of generating idle frequencies in the mixer circuit is separately considered in detail. It is theoretically proven that, unlike balanced mixer circuits that operate on the fundamental harmonic of the local oscillator, in the proposed mixer circuit, oscillations at the image frequency and the sum combination frequency arise as waves with the same field polarization, which propagate in the direction of the signal input of the mixer. In order to use the energy of these waves, a mixer circuit was developed and manufactured, which contained an image rejection filter. Experimental study of this hybrid integrated circuit demonstrated a significant reduction in conversion losses (by approximately 1.5 dB) compared to the circuit without a filter. The parameters of the mixer obtained as a result of the work – conversion losses at the level of 6 dB with the required local oscillator power of the order of 2.5 mW – allow the successful use of the developed hybrid integrated circuit of the mixer as part of millimeter-wave transceivers.

Keywords: balanced subharmonic mixer; millimeter wavelength range; hybrid-integrated circuit; conversion losses

DOI: 10.64915/RADAP.2026.104.23-32

Introduction

Subharmonic mixers represent a special (in a series of such as single-diode, balanced, double-balanced, harmonic, image reject mixers) group, since their use in transceiver's frequency converters involves the use of Local Oscillator (LO) with half (or four times) lower frequency. The attractiveness of such a technical solution is due to the significantly lower (several times) cost of low-frequency generators/synthesizers, as well as the significant advantage of the latter in phase noise level. Although these devices have been proposed and implemented in various designs for a long time, and the industry has ensured their mass production including in the form of separate bulk devices and monolithic integrated circuits [1, 2], interest in their development and improvement of operational characteristics and parameters are still being developed [3,4]. An important reason for this is the rapid advancement of many technologies in the millimeter and submillimeter wavelength ranges, where the relevance of using low-frequency local oscillators in converters becomes absolute. In addition, the advancement to high frequencies necessitates changes to the implementation of subharmonic mixers, which, as a rule, were built according to a scheme that used two diodes connected in antiparallel (the so-called antiparallel diode pair), so that the mixer was essentially a single-diode and required the use of filters in the signal and LO ports. And given that the mixers used a Microstrip Line (MSL) as the electrodynamic basis, the losses in the specified filters at high frequencies became significant, which significantly increased the conversion losses of such mixers. So, the best of them had this parameter at the level of 10 dB [5, 6]. This negatively affects the sensitivity of millimeter-wave receivers in cases where the use of low-noise amplifiers at the input is limited either by their cost or their absence on the market. In this case the input device of the receiver is a mixer, and the noise figure of receiver equals mixer's conversion losses. In several works, systems with significantly lower losses in the millimeter range were used as the electrodynamics system of subharmonic mixers – a suspended microstrip line, an antipodal fin-line. In these cases the best results were obtained regarding conversion losses at the level of 5–6 dB. The results obtained here, however, concern single-diode (in the above-mentioned sense) mixers with filters, i.e. those that involve changes in topology for operation at changed frequencies. The use of a balanced mixer with two diode pairs can provide frequency-independent separation of its heterodyne and signal ports without the use of filters. Hybrid Integrated Circuits (HICs) of balanced mixers operating on the fundamental harmonic of the heterodyne have been successfully used in the millimeter range; the mixers have significant and frequency-independent port separation, and the conversion losses reach theoretical limits (of the order of 3 dB) [7]. At the same time, the number of works devoted to the development of balanced subharmonic mixers is insignificant, and the authors are not aware of any publications describing the HICs of such mixers.

Below, the authors present the results of the study of the proposed design of the subharmonic balanced mixer HIC: the topology of the mixer, the physical foundations of its operation, approximate calculations of diode matching schemes in terms of circuit theory, the results of specifying the dimensions of the elements of the mixer topology in the package of programs for electrodynamic analysis and a comparison of the calculated return loss characteristics with those obtained experimentally. According to the proposed methodology, an analysis of the generation of waves at image and sum frequencies of the mixer was carried out. Based on these results the image enhanced mixer topology was developed. The measurements of the conversion losses and the port's isolation of the sample of mixer demonstrate the advantages of the proposed design.

1 Proposed Topology of the Hybrid Integrated Circuit Mixer

The proposed topology of the HIC mixer is shown in Fig. 1.

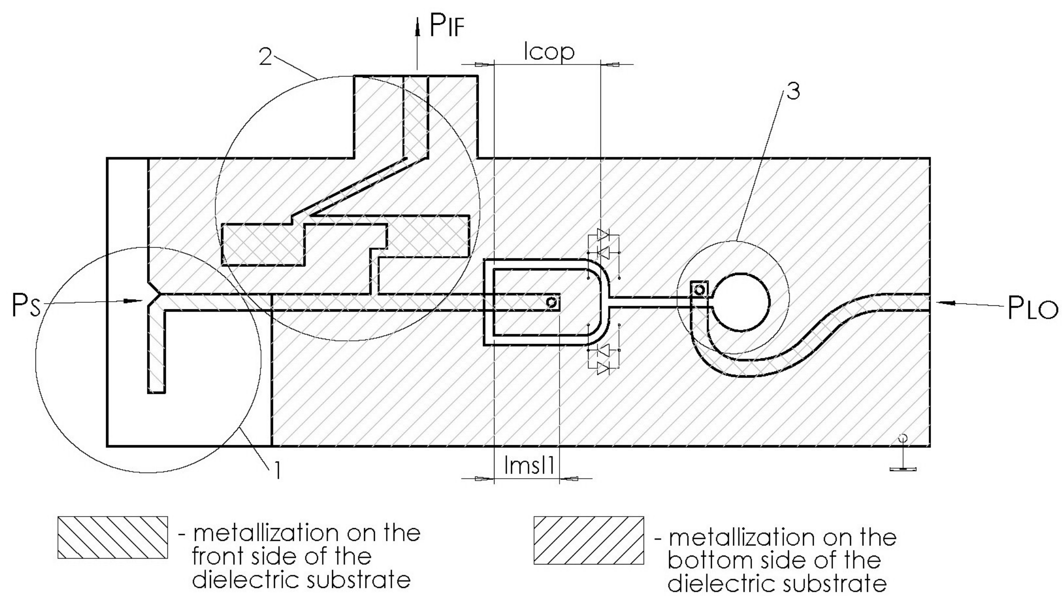

Fig. 1. Hybrid integrated circuit mixer topology; P_{LO} – heterodyne power, P_S – signal power, P_{IF} – intermediate frequency power

As can be seen, the topology is based on a bridge based on a section of a Waveguide-Coplanar Line (WCL), which has been repeatedly used in the designs of balanced mixers on the heterodyne fundamental harmonic. The fundamental difference in this case is that oscillations at the heterodyne frequency are supplied from the side of the WCL, which excites an even-type wave in the WCL, while oscillations at the signal frequency are supplied from the side of the MSL, which excites an odd-type wave in the WCL. The need for this order of excitation is explained by Fig. 2, which depicts the time dependences of the voltages on diodes pairs at the frequencies of the heterodyne (ω_{LO}) and the signal (ω_S), Fig. 2 a,b,c,d. In this case, it is assumed that ω_S=2ω_{LO}, and the voltage values are calculated relative to the grounded metallization layer connecting the ground electrodes of the MSL, WCL and the fins of the fin-line. Fig. 2 e,f show the time dependences of the conductivities of the diode pairs, and Fig. 2 g – the value of the voltage, that appears on the central conductor of the WCL. The dashed line shows the value of this voltage at the output of the intermediate frequency filter. It is obvious that when reversing the mixer ports to the opposite, there will be no voltage at the output of the intermediate frequency filter since the values of the voltages on the diodes at the signal frequency will be opposite.

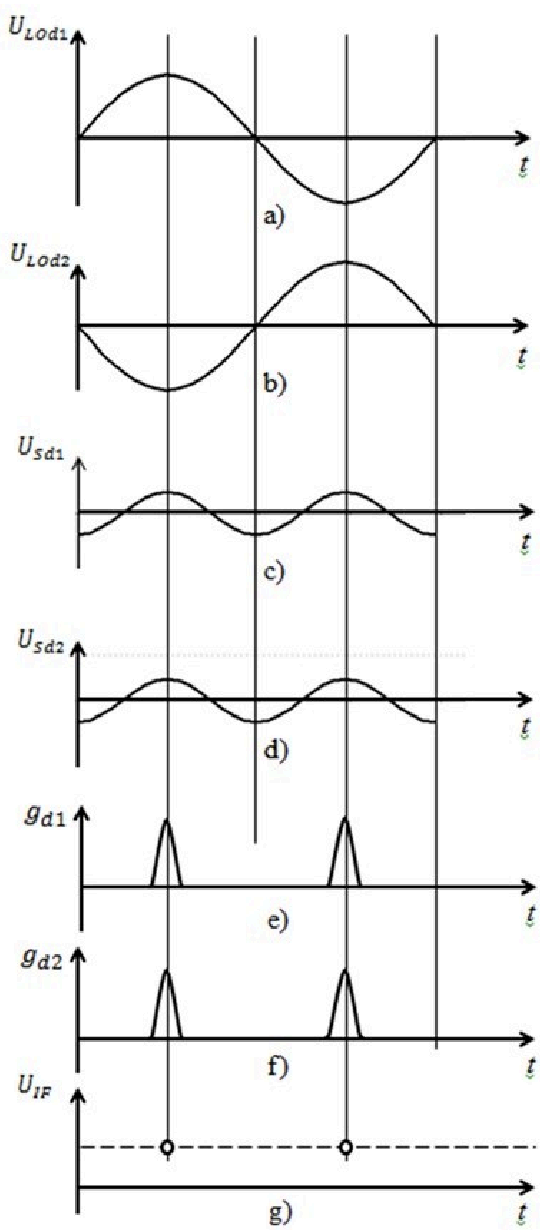

Fig. 2. Time dependences of voltages on diode pairs

The mixer HIC contains additional elements: elements 1 form a longitudinal probe transition from a rectangular waveguide to the MSL; elements 2 form a Low-Pass Filter (LPF) on the MSL segments; elements 3 form a transition from the input MSL in the mixer *LO* port to the fin-line.

2 Preliminary Calculation of the Mixer Topology Elements in Terms of the Long Lines Theory

The specified features of the topology, in particular, the excitation of the WCL from the fin-line side under the condition of an excitation frequency that is half the signal frequency, force us to pay special attention to the topology of the fin-line and WCL, in particular, to the widths of the slots of these lines. Fig. 3–5 shows the frequency dependences of the slowing factor and line impedance of the fin-line (Fig. 3) and WCL (Fig. 4, 5) for different values of the slot width w and several values of the distance between the slots in the WCL, calculated in accordance with [13]. The calculations were made for lines made on a dielectric substrate with a thickness of $d = 254\ \mu$ with a dielectric constant $\varepsilon = 2.2$. It should also be noted that the width of the WCL slots is chosen to be fixed ($w = 150\ \mu$), which meets the technological requirements for the design of the selected diodes with beam terminals. The cross-section of the waveguide is $a \times b = 11 \times 5.5$ mm, with a cutoff frequency $f_c = 13.63$ GHz. A subharmonic mixer operating in this operating frequency range of such a waveguide (18–26 GHz) should have a WCL cutoff frequency on an even-type wave no higher than approximately 8 GHz (for the necessary deviation from the critical frequency of 1 GHz). From Fig. 4, however, it is clear that for the used parameters of the WCL topology, its operating range begins with frequencies only slightly below 9 GHz (the exact value of the cutoff frequency at $dpr = 1.3$ mm is 8.69 GHz), which limits the operating range of this mixer to the minimum frequency $f_{min} \approx 19.5$ GHz. A simplified calculation of the main elements of the topology will be demonstrated on the example of developing a mixer with an operating frequency range for the input signal $f_{min} = 21.7$ GHz, $f_{max} = 22.3$ GHz, and a LO frequency $f_{LO} = 10.5$ GHz. We use diode pairs of the MA4E2039 type (MACOM).

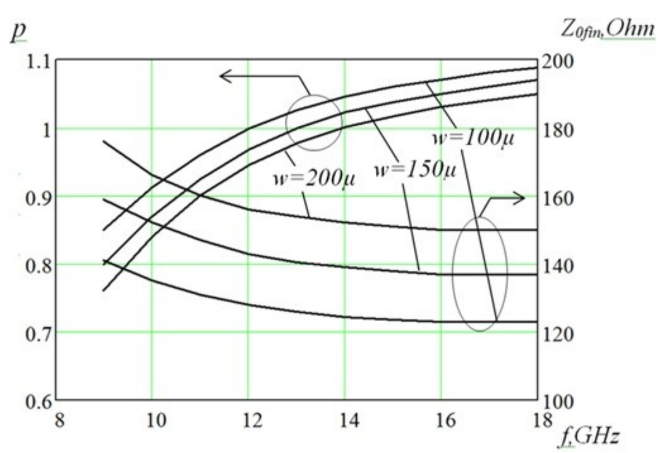

Fig. 3. Frequency dependences of fin-line slowing factor and line impedance

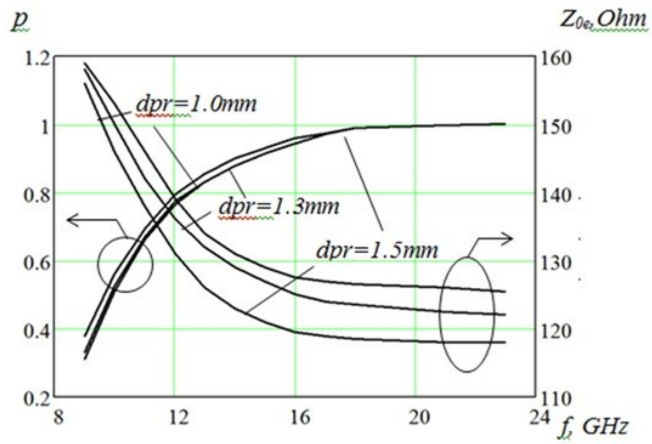

Fig. 4. Frequency dependences of WCL slowing factor and line impedance; even type. Here and below *dpr* is the distance between the slots of WCL

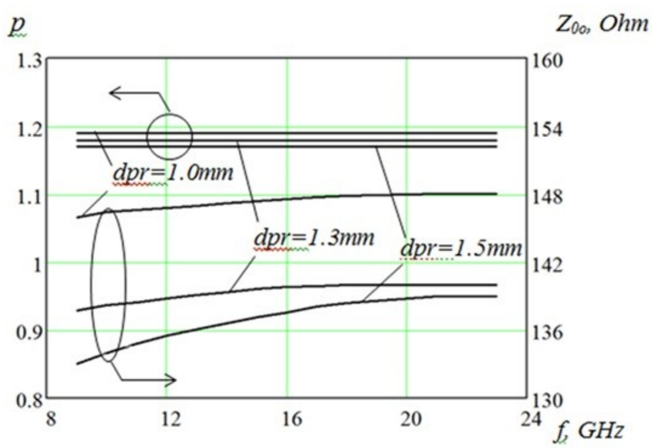

Fig. 5. Frequency dependences of WCL slowing factor and line impedance; odd type

The parameters of the simplified equivalent circuit of diodes were measured experimentally in the fin-line using the method proposed by the authors, which provides automatic setting of the position of the reference plane [8]. It was found that the diode is a parallel connection of the active resistance $R_d = 55$ Ohm and the capacitance $C_d = 0.055$ pF. The equivalent circuit of the mixer unit at the *LO* frequency is shown in Fig. 6

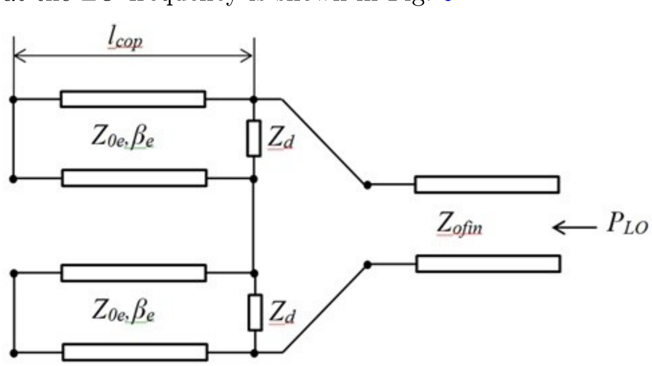

Fig. 6. Equivalent circuit of a mixer unit at the *LO* frequency

Using the data in Fig. 4, we find the length of the WCL section from the relation:

$$l_{cop} = 1\frac{1}{\beta_e}\arctan\left(\frac{1}{2\pi f_{LO} C_d Z_{0e}}\right) = 0.7 \text{ cm}.$$

Since the effective short-circuit plane of the WCL slots is located on the longitudinal axis of the mixer topology (Fig. 1), and the diodes are installed with their electrodes at the edges of the WCL slot (Fig. 1), we correct the found size lcop by the width of the central conductor of the WCL, which in this case is $dpr = 1.3$ mm. Therefore, for further use, we use the value $l_{cop} = 5.7$ mm. We choose the width of the WCL slot equal to $w_{fin} = 100\ \mu$ – a value that is the technological limit for obtaining this parameter with the required accuracy in production. In this case (Fig. 3) $Z_{0fin} = 132$ Ohm. The calculated frequency dependence of the VSWR of the considered node is shown in Fig. 7. The equivalent circuit of the node with diodes at the signal frequency is shown in Fig. 8. When constructing the circuit, an equivalent representation of the excitation node of the WCL on an odd-type wave by a microstrip line from the side of the signal port was used. Obviously, we have:

$$Z_{in} = jZ_{0MSL1}\tan\beta_{MSL1} l_{MSL1} + \frac{1}{2Y_{in}}, \qquad (1)$$

where

$$Y_{in} = Y_{0e}\frac{Y_d + jY_{0e}\tan\beta_e l_{cop}}{Y_{0e} + jY_d\tan\beta_e l_{cop}},$$

Y_d – conductivity of the diode pair; Z_{0MSL1}, β_{MSL1} – line impedance and phase constant of the MSL section with length l_{MSL1} (Fig. 1).

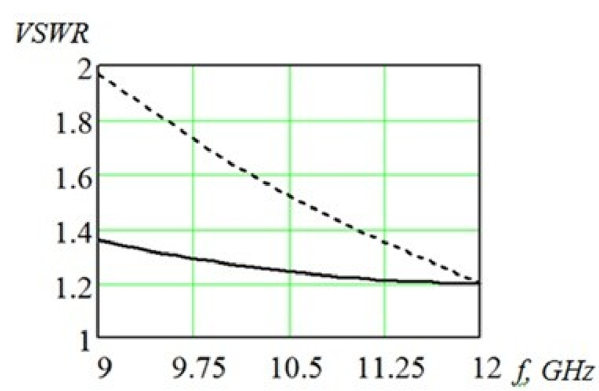

Fig. 7. Calculated frequency dependence of the VSWR from the *LO* node (dashed curve – the result of the analysis in CST)

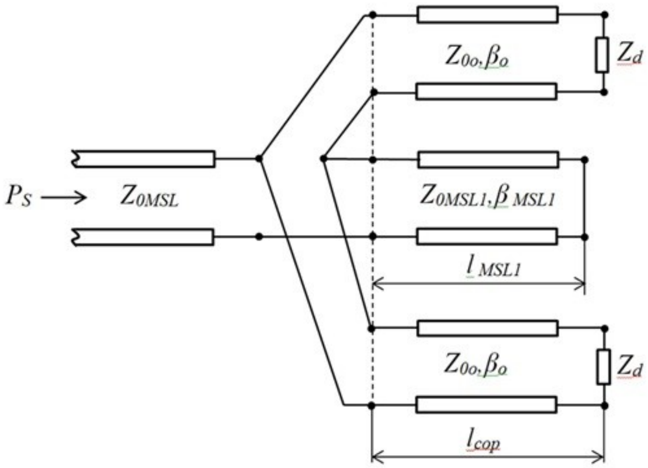

Fig. 8. Equivalent circuit of a mixer unit at the signal frequency; β_o – phase constant of the odd-type wave in WCL

The first term in (1) is the input impedance of a short-circuited microstrip loop, which compensates for the reactive component of the input impedance of the WCL at the point of its connection. In this case, this reactance turned out to be capacitive. Therefore, a short short-circuited loop was required for compensation, which, by the way, simultaneously ensures the connection of the intermediate frequency current of the IF mixer (Fig. 1). Calculations according to (1) give the value of the length $l_{MSL1} = 0.8$ mm; while the active component of the input impedance is as low as $Re(Z_{in}) = 25$ Ohm. And since with such a wave impedance of the MSL, its width turns out to be greater than the width of the central section of the WCL, the resistance of the microstrip loop line was taken larger in magnitude, $Z_{0MSL1} = 50$ Ohm. In this case, the width of the loop line is 0.77 mm, and its length is 0.84 mm. Fig. 9 shows the calculated frequency dependence of the VSWR from the signal input side.

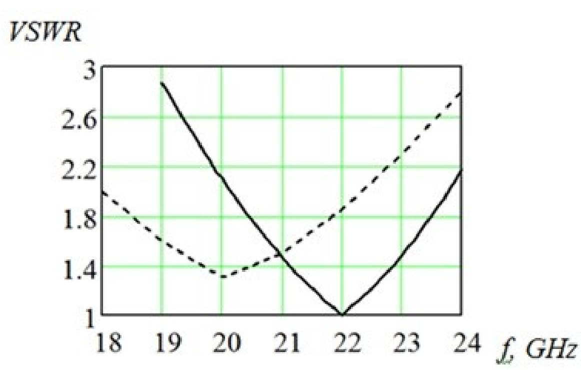

Fig. 9. Calculated frequency dependence of the VSWR from signal node (dashed curve – the result of the analysis in CST)

It should be noted that in the case of inductive nature of the input resistance at the point of connection of the WCL, reactance compensation is achieved by connecting a short open loop. In this case, the output of the IF voltage can be implemented using a wire half-turn, which is connected to the central conductor of the WCL, and the other end to the second capacitive element of the LPF path of the intermediate frequency.

3 Results of Optimization of Dimensions in the Electrodynamic Analysis Software Package

The obtained results were used for their refinement in the electrodynamics analysis software package CST Microwave Studio. The calculated frequency dependences of the VSWR for the mixer with the dimensions found above are shown in Fig. 7 for the LO, and Fig. 9 – for the signal ports by dashed lines. Comparison of the results shown demonstrates the usefulness of approximate calculations of dimensions, which now only require optimization. As a result of optimization of dimensions, the minimum value of the VSWR at the central frequency of the operating frequency range of the input signal was obtained when the length l_{cop} of the central conductor of the WCL was reduced: $l_{cop} = 3.8$ mm; $l_{MSL1} = 1.8$ mm. The frequency dependences of the VSWR from the mixer inputs are shown in Fig. 10.

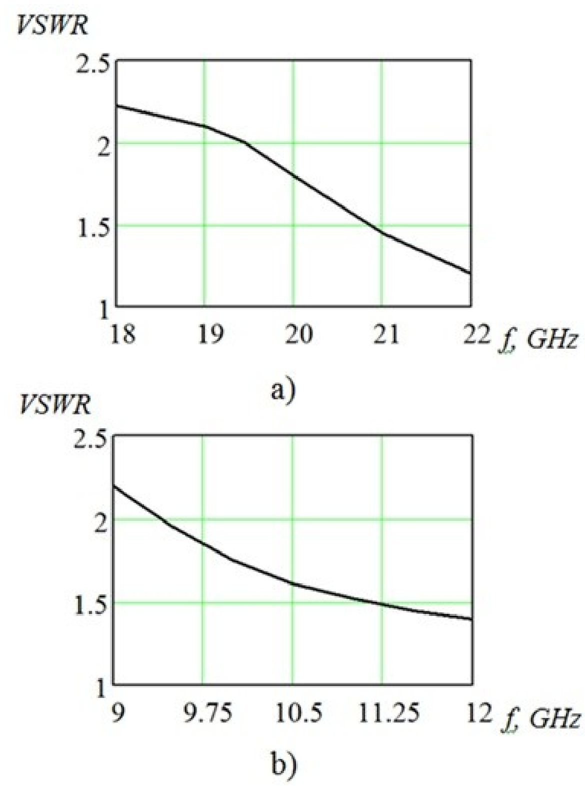

Fig. 10. Frequency dependences of the VSWR from the mixer inputs, optimization results: a) signal input, b) LO input

As can be seen, the required shift of the minimum reflection from the side of the signal port of the mixer is achieved by some reduction in the length l_{cop}. This contributes to a reduction in the linear dimensions of the mixer, as well as a reduction in the capacitance of the first element of the low-pass filter path of the IF, which determines the cutoff frequency of this filter. Fig. 11, 12 present the results of calculations of the parameters of the auxiliary elements of the mixer: Fig. 11 – longitudinal-probe transition to the MSL from the side of the rectangular waveguide to the signal port (position 1 in Fig. 1); Fig. 12 – transition to the fin-line from the MSL to the LO port (position 3 in Fig. 1).

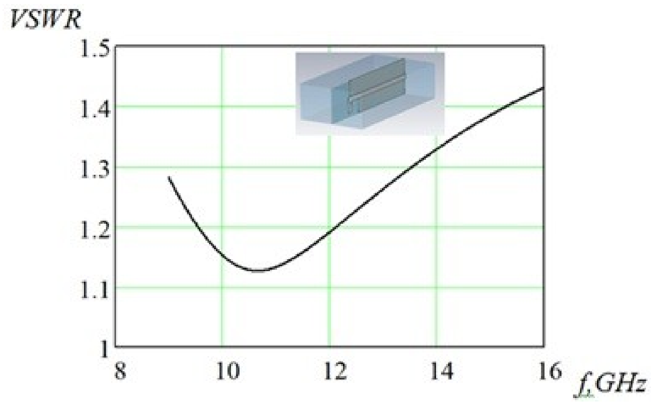

Fig. 11. Characteristics of the longitudinal-probe transition to the MSL

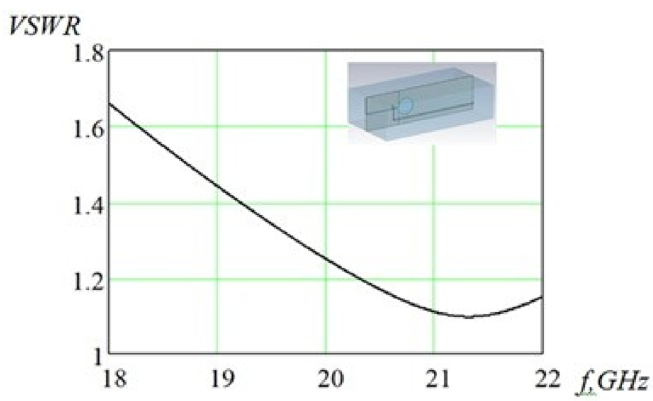

Fig. 12. Characteristics of the transition to the fin-line from the MSL in the LO port

The results of the experimental study of the manufactured mixer sample (photo in Fig. 13, the LO input and intermediate frequency output are made via standard SMA connectors) are presented in Fig. 14–17. The frequency dependences of the VSWR from all three ports are shown in Fig. 14.

The measured isolation between the LO and IF ports is shown in Fig. 15. Fig. 16 shows the frequency dependence of the conversion losses, and Fig. 17 shows the dependence of the conversion losses on the LO power.

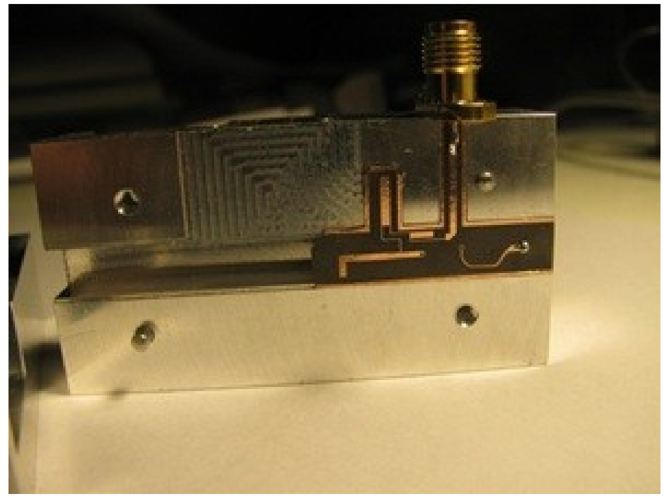

Fig. 13. Mixer sample

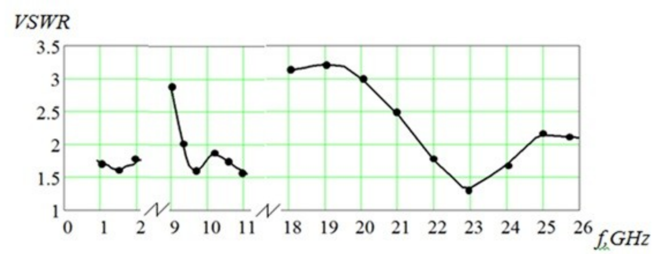

Fig. 14. Frequency dependence of the VSWR from the mixer inputs

The obtained results regarding the conversion losses correspond to the level considered high for similar devices. We especially note the ultra-low required level of LO power (about 3 mW), which is much lower than the values for the samples known from the literature, as well as for those produced by the industry (for example, 30 mW for MAMX-011009, MACOM, HMC-MDB 218, Analog Devices [14]).

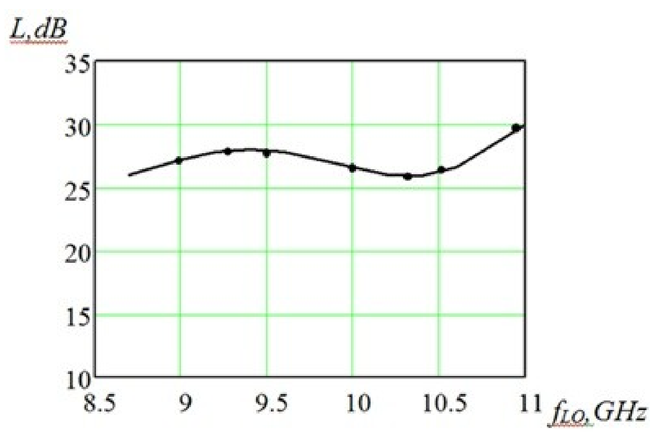

Fig. 15. Frequency dependence of the isolation between LO and IF ports

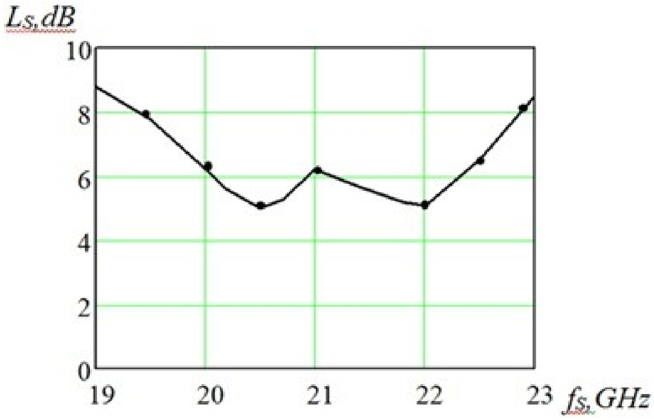

Fig. 16. . Frequency dependence of conversion losses at fixed $f_{IF} = 1.3$ GHz; $P_{LO} = 2.7$ mW

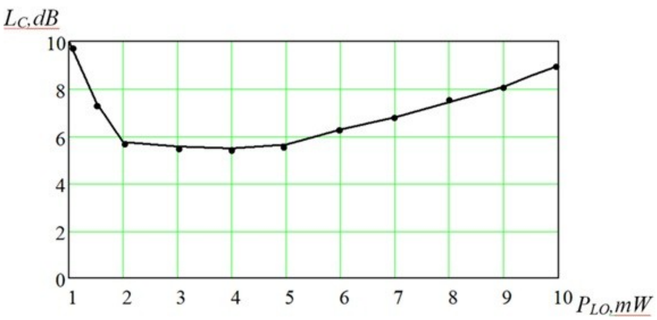

Fig. 17. Dependence of conversion losses on LO power; $f_S = 22.5$ GHz; $f_{LO} = 10.6$ GHz

Thus, the developed mixer meets the high requirements for conversion losses, the level of isolation between the ports, and the required level of LO power. The specified characteristics were provided by a topology that does not require the use of filters at the signal and LO inputs of the mixer. The mixer, designed as a hybrid integrated circuit, provides flexibility in its application as part of complex millimeter-wave devices made on one substrate. This advantageously distinguishes it from similar connectorized devices produced by industry [11, 12].

4 Using Idle Conversion Frequencies to Reduce Conversion Losses

It is well known that the use of idle mixer frequencies allows to significantly reduce conversion losses [9, 10]. Theoretical analysis of their influence on the parameters has been performed in numerous works. For analysis, current flow circuits are selected for each of the frequencies under consideration, and the interaction between them occurs in the selected nonlinear part of the mixer circuit. This approach allows us to calculate the value of the conversion losses, the equivalent resistance of the intermediate frequency source, the influence of loads on the idle frequencies of the mixer, etc. Since such an analysis is very laborious, we limit ourselves here to questions of a qualitative nature, namely: in which ports of the considered subharmonic balanced mixer and at which frequencies do idle frequencies of the conversion occur, which take away part of the power of the input signal. So, their return to the conversion process can reduce the conversion losses of the mixer. With this formulation of the question, the mixer circuit can be simplified to the form shown in Fig. 18, and its analysis is carried out by the method of successive approximations.

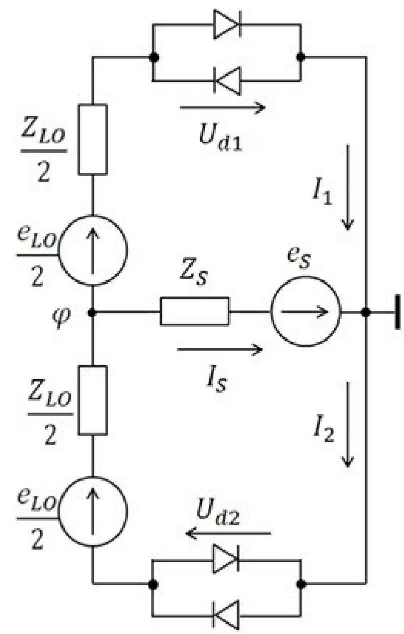

Fig. 18. Simplified diagram of the mixer

The essence of the method is to isolate some small parameter, and the solution to the problem is sought in the form of an expansion into a series of its powers. From the well-known expression for the $I-V$ characteristic of an antiparallel diode pair, we have:

$$I_d = I_s\left(e^{\dfrac{\alpha U_d}{kT}} - 1\right) - I_s\left(e^{-\dfrac{\alpha U_d}{kT}} - 1\right) = \\ = 2I_s \operatorname{sh}\left(\frac{\alpha U_d}{kT}\right), \quad (2)$$

where U_d – voltage across a diode pair.

From here we find

$$U_d = \frac{kT}{\alpha} \operatorname{arsh}\left(\frac{I_d}{2I_s}\right). \quad (3)$$

From (2), (3) we can find the differential conductivity

$$g_d = \frac{\partial I_d}{\partial U_d} = \frac{2I_s\alpha}{kT} \operatorname{ch}\left(\frac{\alpha U_d}{kT}\right) \quad (4)$$

and the differential resistance of the diode pair

$$R_d = \frac{\partial U_d}{\partial I_d} = \frac{kT}{2I_s\alpha}\frac{1}{\sqrt{1+\left(\frac{I_d}{2I_s}\right)^2}}. \tag{5}$$

The coefficient α/kT in (1) is of the order of 0.8 V^{-1}, and the value of I_s for diodes with a Schottky barrier is less than 10^{-6} A. Therefore the expansion in a series of powers of the conductivity voltage U_d according to (3) will lead to its rapid convergence:

$$\begin{gathered} g_d \approx G_0 + \beta {U_d}^2; \quad G_0 = \frac{2I_s\alpha}{kT}; \\ \beta - \text{small value}, \quad \beta = \frac{1}{2}G_0\frac{\alpha}{kT}. \end{gathered} \tag{6}$$

On the contrary, the expansion of (4) in powers of $\left(\frac{I_d}{2I_s}\right)^2$ does not lead to convergence of the series. Accordingly, the analysis of the circuit in Fig. 19 will be carried out by the method of nodal potentials, according to which we have:

$$\begin{gathered} I_1\frac{Z_{LO}}{2} + U_{d1} = \varphi + \frac{e_{LO}}{2}, \\ I_2\frac{Z_{LO}}{2} + U_{d2} = -\varphi + \frac{e_{LO}}{2}, \\ I_1 = U_{d1}\cdot g_{d1}, \qquad I_2 = U_{d2}\cdot g_{d2}, \\ I_s + I_1 = I_2. \end{gathered} \tag{7}$$

Hence, using (6), we obtain:

$$\begin{aligned} &\varphi_1\left(G_0\frac{Z_{LO}}{2}+1\right) = e_{LO} - 0.125\beta Z_{LO}\left(\varphi_1^3 + 3\varphi_1\varphi_2^2\right), \\ &\varphi_2\left(G_0\left(\frac{Z_{LO}}{2}+2Z_S\right)+1\right) = \\ &= -2e_s - 0.25\beta\left(\frac{Z_{LO}}{2}+2Z_S\right)\left(3\varphi_1^2\varphi_2 + \varphi_2^3\right), \end{aligned} \tag{8}$$

where $\varphi_1 = U_{d1} + U_{d2}$; $\varphi_2 = U_{d1} - U_{d2}$.

The nonlinear system of equations (8) is solved by the method of successive approximations, setting $\varphi_{1,2} = \varphi_{1,2}^{(0)} + \varphi_{1,2}^{(1)} + \varphi_{1,2}^{(2)} + \ldots$, where successive values of $\varphi_{1,2}^{(i)}$ are proportional to the increasing power of the small parameter β. Substituting successively the solution in the general form into (8) and equating terms of the same order of smallness on both sides of the equations, we obtain:

$$\begin{aligned} \varphi_1^{(0)} &= \frac{e_{LO}}{G_0\frac{Z_{LO}}{2}+1}; \\ \varphi_2^{(0)} &= -\frac{2e_C}{G_0\left(\frac{Z_{LO}}{2}+2Z_C\right)+1}; \\ \varphi_1^{(1)} &= -\beta\frac{0.125Z_{LO}\varphi_1^{(0)3}}{G_0\frac{Z_{LO}}{2}+1}; \\ \varphi_2^{(1)} &= -\beta\frac{0.125\left(\frac{Z_{LO}}{2}+2Z_S\right)\left(\varphi_1^{(0)2}\varphi_2^{(0)}\right)}{G_0\left(\frac{Z_{LO}}{2}+2Z_S\right)+1}; \\ \varphi_1^{(2)} &= -\beta\frac{0.375Z_{LO}}{G_0\frac{Z_{LO}}{2}+1}\varphi_1^{(0)2}\varphi_1^{(1)}; \\ \varphi_2^{(2)} &= -\beta\frac{1.5\left(\frac{Z_{LO}}{2}+2Z_S\right)}{G_0\left(\frac{Z_{LO}}{2}+2Z_S\right)+1}\varphi_1^{(0)}\varphi_1^{(1)}\varphi_2^{(0)}. \end{aligned} \tag{9}$$

From (9) it is clear that successive values of $\varphi_{1,2}^{(i)}$ contain factors proportional to the values of the power β: for example, $\varphi_1^{(2)} \sim \beta\varphi_1^{(0)2}$, $\varphi_2^{(1)} \sim \beta^2\varphi_1^{(0)2}\varphi_2^{(0)}$ etc.

Analyzing the circuit in Fig. 18, we note that the variable φ_1 is responsible for the voltage at which the diode pairs are connected in series, i.e. in the direction of the field of the even-type wave in the WCL (Fig. 1), while φ_2 is responsible for the field of the odd-type in this line. Let us now assume that the fields in these waves are proportional to $\cos(\omega_{LO}t)$ and $\cos(\omega_S t)$. In the first approximation, we have the generation of the third harmonic of the LO frequency on the even-type wave, as well as the excitation of oscillations at the intermediate frequency $(\omega_{IF} = 2\omega_{LO} - \omega_S)$ and the sum combination frequency $(2\omega_{LO} + \omega_S)$ on the odd-type wave. In the second approximation, waves at frequencies $3\omega_{LO}$, $5\omega_{LO}$ are excited by an even-type WCL wave, in particular, a wave at frequency $|4\omega_{LO} - \omega_S| = |2\omega_{LO} + (2\omega_{LO} - \omega_S)| = 2\omega_{LO} + \omega_{IF}$ – the image frequency of conversion into waves of odd-type WCL.

Thus, it was established that, unlike a conventional balanced mixer, in which waves at the frequencies of the image channel of conversion and the sum combination frequencies are excited by the mixer on waves of different types, in the mixer under consideration, waves at both frequencies are generated as waves of odd-type of WCL – waves with the same field polarization.

Fig. 19 shows the results of measurements of the dependence of the mixer conversion losses on the relative phase angle of the reflection coefficient from a specially made band-pass filter (BPF) of the image channel placed at the signal input of the mixer. The BPF had losses of the order of 0.15 dB, while the attenuation at the image channel frequency $f = 19.9$ GHz was 16 dB. A significant reduction in conversion losses (up to 4.85 dB versus 6.00 dB at a matched load at the image channel frequency) indicates the feasibility of including such BPF in the mixer's HIC.

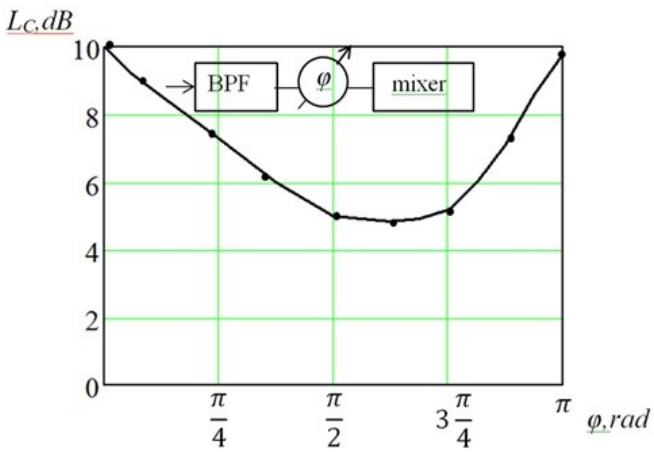

Fig. 19. Dependence of conversion losses on the relative phase angle

The used BPF with a quarter-wave coupling had losses in the signal frequency band of less than 0.8 dB. The measured frequency dependence of the attenuation of this BPF is shown in Fig. 20; here the solid curve shows this dependence, calculated in CST Microwave Studio. The optimal distance of the filter to the WCL section of the mixer was found experimentally. Fig. 21 shows the results of measurements of conversion losses in the signal frequency band.

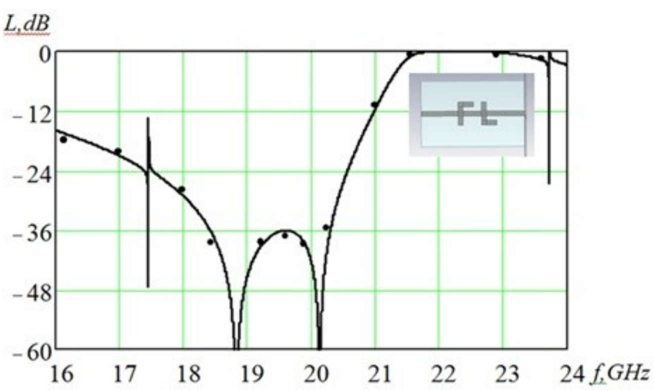

Fig. 20. Frequency dependence of the attenuation of the manufactured BPF

It can be seen that the obtained results are comparable to those typical for HIC of balanced mixers operating on the fundamental harmonic of a *LO*. According to this parameter, the developed HIC meet the requirements for modern input devices of the millimeter wavelength range.

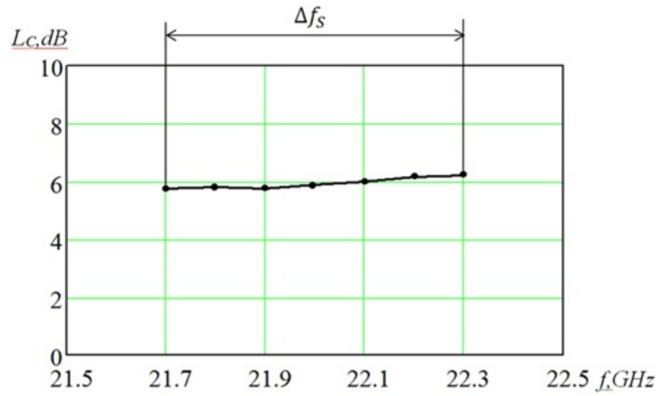

Fig. 21. Measured conversion losses of a mixer with a BPF

Conclusion

The proposed and investigated in the work new topological solution for the HIC of the balanced subharmonic mixer revealed a number of features that make it promising for inclusion it in budget and, at the same time, high-quality transceivers of the millimeter wavelength range. Among them – a low level of conversion losses and a very low level of the required *LO* power. These parameters are often considered critical when designing these devices.

References

[1] WR15SHM. Sub-Harmonic Mixer (SHM), *VDI*.

[2] MAMX-011009. Sub-Harmonic Pumped Mixer 14-32GHz Rev.V1, *Macom*.

[3] H. Li, X. Gao, X. Bu, H. Liu and J. An. (2023). The Design Methods and Experiments for a 220-GHz Quasi-Optical Cryogenic Schottky Subharmonic Mixer of High Performance. *IEEE Transactions on Microwave Theory and Techniques*, vol. 71, no. 7, pp. 2897-2908, doi:10.1109/TMTT.2023.3238814.

[4] H. Li, X. Gao, D. Qiao, Z. Chen, X. Bu and J. An. (2025). A 220-GHz Cryogenic Quasi-Optical Schottky Subharmonic In-Phase Quadrature Demodulation Receiver. *IEEE Transactions on Microwave Theory and Techniques*, vol. 73, no. 3, pp. 1473-1486, doi:10.1109/TMTT.2024.3447762.

[5] C. -H. Lin, Y. -A. Lai, J. -C. Chiu and Y. -H. Wang. (2007). A 23–37 GHz Miniature MMIC Subharmonic Mixer. *IEEE Microwave and Wireless Components Letters*, vol. 17, no. 9, pp. 679-681, doi:10.1109/LMWC.2007.903460.

[6] H. Okazaki and Y. Yamaguchi. (1997). Wide-band SSB subharmonically pumped mixer MMIC. *IEEE Transactions on Microwave Theory and Techniques*, vol. 45, no. 12, pp. 2375-2379, doi:10.1109/22.643847.

[7] B. Boukari, E. Moldovan, S. Affes, K. Wu, R. G. Bosisio and S. O. Tatu. (2007). A Low-Cost Millimeter-Wave Six-Port Double-Balanced Mixer. *International Symposium on Signals, Systems and Electronics*, Montreal, QC, Canada, pp. 513-516, doi:10.1109/ISSSE.2007.4294525.

[8] Yu. O. Khokhanovska and M. Yu. Omelianenko. (2018). The measurement of the p-i-n diodes parameters in the fin-line in the millimeter wave region. *Visnyk NTUU KPI Seriia - Radiotekhnika Radioaparatobuduvannia*, no. 75, pp. 5-8. DOI:10.20535/RADAP.2018.75.5-8.

[9] Yanfeng Xu, (2008). A low conversion loss millimeter wave fourth subharmonic mixer. *International Conference on Microwave and Millimeter Wave Technology*, Nanjing, China, pp. 843-845, DOI: 10.1109/ICMMT.2008.4540532.

[10] J. Xu, Z.-B. Xu, J. Guo, C. Qian and D.-X. Zhao. (2021). A broadband millimeter-wave sub-harmonic mixer using microstrip passive circuits. *Journal of Infrared and Millimeter Waves*, 40(1): 33.

[11] Eravant. SUBHARMONICALLY PUMPED MIXERS, *Eravant*.

[12] ZAX MILLIMETER WAVE CORPORATION. *zaxmmw*.

[13] Bharathi Bhat and Shiban K. Koul. (1987). Analysis, Design and Applications of Fin Lines. Artech House. *Artech House*, 486 p.

[14] GaAs MMIC SUB-HARMONIC IRM MIXER, 54–64 GHz. HMC-MDB218. *Analog Devices*.

Гібридно-інтегральний балансний субгармонічний змішувач міліметрового діапазону з малими втратами перетворення

Омеляненко М. Ю., Романенко Т. В., Туреєва О. В.

В роботі всебічно досліджено запропоновану топологію гібридно-інтегральної схеми балансного субгармонічного змішувача, ефективну при використанні у міліметровому діапазоні довжин хвиль. Детально висвітлено принцип роботи змішувача, запропоновано його модель у термінах теорії довгих ліній, на базі якої у першому наближенні розраховано розміри елементів топології інтегральної схеми. Уточнення розмірів проведено в програмі електродинамічного аналізу CST MicrowaveStudio. За результатами розрахунків було виготовлено зразки змішувачів і проведено їх експериментальне дослідження. Окремо детально розглянуто процес генерації холостих частот у змішувачі. Теоретично доведено, що, на відміну від балансних змішувачів, які працюють на основній гармоніці гетеродина, у запропонованому змішувачі коливання на частоті дзеркального каналу прийому і сумарній комбінаційній частоті виникають як хвилі з однаковою поляризацією поля, які поширюються в напрямку сигнального входу змішувача. З метою використання енергії зазначених хвиль був розроблений і виготовлений змішувач, який містив фільтр дзеркального каналу. Експериментальне дослідження цієї гібридно-інтегральної схеми продемонструвало суттєве зменшення втрат перетворення (приблизно на 1.5 дБ) порівняно зі схемою без фільтра. Отримані в результаті роботи параметри змішувача – втрати перетворення на рівні 6 дБ при необхідній потужності гетеродина порядку 2.5 мВт – дозволяють з успіхом використати розроблений гібридно-інтегральний змішувач в складі прийомопередавачів міліметрового діапазону довжин хвиль.

Ключові слова: балансний субгармонічний змішувач; міліметровий діапазон довжин хвиль; гібридно-інтегральна схема; втрати перетворення